Black Currant Phytoconstituents Exert Chemoprevention of Diethylnitrosamine-Initiated Hepatocarcinogenesis by Suppression of the Inflammatory Response

Anupam Bishayee,[1]* Roslin J. Thoppil,[2] Animesh Mandal,[2] Altaf S. Darvesh,[2] Vahagn Ohanyan,[3] J. Gary Meszaros,[3] Erzsébet Háznagy-Radnai,[4] Judit Hohmann,[4] and Deepak Bhatia[2]

[1]*Department of Pharmaceutical and Administrative Sciences, School of Pharmacy, American University of Health Sciences, Signal Hill, California*
[2]*Cancer Therapeutics and Chemoprevention Group, Department of Pharmaceutical Sciences, College of Pharmacy, Northeast Ohio Medical University, Rootstown, Ohio*
[3]*Department of Integrative Medical Sciences, College of Medicine, Northeast Ohio Medical University, Rootstown, Ohio*
[4]*Department of Pharmacognosy, University of Szeged, Szeged, Hungary*

Black currant fruits containing high amounts of anthocyanins are known to possess potent antioxidant and anti-inflammatory properties. We have previously reported that anthocyanin-rich black currant skin extract (BCSE) inhibits diethylnitrosamine (DENA)-initiated hepatocarcinogenesis in rats although the underlying mechanisms are not fully understood. Our present study investigates the anti-inflammatory mechanisms of BCSE during DENA rat liver carcinogenesis. Dietary BCSE (100 or 500 mg/kg) treatment for 22 wk afforded a striking inhibition of DENA-induced hepatic gamma-glutamyl transpeptidase-positive preneoplastic foci in a dose-responsive fashion. There was a significant increase in hepatic expression of heat shock proteins (HSP70 and HSP90), cyclooxygenase-2, and nuclear factor-κB (NF-κB) in DENA-exposed rat livers. Dietary BCSE dose-dependently abrogated all these elevated inflammatory markers. The possible cardiotoxicity of BCSE was assessed by monitoring cardiac functions using transthoracic echocardiography. BCSE-mediated anti-inflammatory effects during rat liver carcinogenesis have been achieved without any cardiotoxicity. Our results provide convincing evidence, for the very first time, that suppression of the inflammatory cascade through modulation of the NF-κB signaling pathway could be implicated, at least in part, in the chemopreventive effects of black currant bioactive phytoconstituents against experimental hepatocarcinogenesis. These results coupled with an excellent safety profile of BCSE support the development of black currant phytochemicals for the chemoprevention of inflammation-driven hepatocellular cancer.

Key words: hepatocarcinogenesis; inflammation; chemoprevention; nuclear factor-κB signaling; cyclooxygenase-2; heat shock proteins

INTRODUCTION

Cancer has progressed to surpass most chronic diseases to be the leading cause of mortality in both the developed and developing world [1]. Diagnosed as the 5th most common cancer worldwide, liver cancer represents the second most frequent cause of cancer death [2]. Hepatocellular carcinoma (HCC) qualifies as the major subtype affecting the population of liver cancer patients, mostly in east and south-east Asia as well as in middle and western Africa [2,3]. Increase in liver cancer incidence has been witnessed all over the world including central and western Europe as well as north America [4–6]. The United States too has reported more than 70% increase in the incidence of HCC in the last 25 yr [7]. HCC arises from underlying viral infections, such as hepatitis B and hepatitis C, and alcoholic cirrhosis; however, beyond these triggering factors, chronic oxidative stress and inflammation play a pivotal role in adding insult to injury, ultimately resulting in a full-blown condition of liver cancer. In addition to these insults, metabolic disorders (obesity), autoimmune hepatitis as well as environmental and dietary exposure to carcinogens, including aflatoxins and nitrosamines, contribute to HCC occurrence [8–11]. Liver transplantation and surgical resection serve as current curative treatments while

Abbreviations: HCC, hepatocellular carcinoma; BCSE, black currant skin extract; DENA, diethylnitrosamine; PB, phenobarbital; GGT, gamma-glutamyl transpeptidase; HSP, heat shock protein; COX-2, cyclooxygenase-2; NF-κB, nuclear factor-kappaB; HRP, horse radish peroxidase; PCR, polymerase chain reaction.

*Correspondence to: Department of Pharmaceutical and Administrative Sciences, School of Pharmacy, American University of Health Sciences, 1600 East Hill Street, Signal Hill, CA 90755.

Received 16 October 2011; Revised 22 November 2011; Accepted 30 November 2011

DOI 10.1002/mc.21860

Published online in Wiley Online Library (wileyonlinelibrary.com).

radiofrequency ablation, chemoembolization, and intrahepatic radiotherapy are referred to as palliative treatments; both of these treatments, however, come with heavy limitations and often do not qualify as options for a large majority of patients. The only drug approved by the United States Food and Drug Administration for the treatment of HCC is the multikinase inhibitor sorafenib which has been indicated to produce adverse effects while its only marked benefit is an increase in median survival time of 9.2 months [12]. In light of such dismal therapeutic options a winning concept lies in the idea of chemoprevention.

Chemoprevention can be defined as an emerging strategy to prevent, reduce, slow, or reverse the occurrence and progression of cancer by the administration of one or more naturally occurring or synthetic compounds [13–16]. Fruits, especially berries, are abundant in the antioxidant flavonoids, phenolic acids, vitamins as well as carotenoids, tannins, lignans, and stilbenes [17–20]; all of which have shown to possess potent chemopreventive effects as well as various other health benefits [21–23]. Black currant (*Ribes nigrum* L.) berries, widely grown in Europe, New Zealand, and Northern Asia in cooler weather conditions [24], are particularly rich in the flavanoid antioxidant anthocyanins (250 mg/100 g fresh fruit) [25–27], and also known to contain various other antioxidant phenolics, including flavanoids and phenolic acids [28]. Anthocyanins are the water soluble pigments that confer the vibrant colors of red, violet, blue, and purple shades to the various plants and especially differently colored berries, including strawberries, blueberries as well as in beets and cabbage [29]. Coined by Lister et al. [30] as ''*superfruits*,'' black currants are known to exhibit free radical scavenging properties through the potent antioxidant mechanisms [31]. Emerging studies, both preclinical and clinical, have identified several constituents of black currant fruits to exert anti-inflammatory, antimicrobial, immunostimulatory, and immunomodulatory effects [24,32–37].

Various in vitro studies conducted using various cancer cell lines originating from the breast, colon, stomach, and prostate have firmly established the anticarcinogenic, antiproliferative, antitumor, and cytotoxic effects of black currant constituents [38–40]. Recently, an in vitro study from our laboratory [41] show the antiproliferative effects of an anthocyanin-rich black currant fraction against HepG2 human liver cancer cells which confirm the results reported from other laboratories [42–44]. As there are only two preclinical animal studies reporting antitumor effects of black currant products [45,46], our laboratory conducted a novel chemopreventive study utilizing dietary anthocyanin-rich black currant skin extract (BCSE) against diethylnitrosamine (DENA)-initiated and phenobarbital (PB)-promoted hepatocarcinogenesis in rats. Significant chemopreventive effects were observed with BCSE treatment which dose-dependently reduced the incidence, total number, and multiplicity of visible hepatocyte nodules by antiproliferative and proapoptotic mechanisms through the upregulation of Bax and downregulation of Bcl-2 expressions [47]. The results of our previous study [48] provided significant evidence suggesting anthocyanin-rich black currants abrogate oxidative stress through the activation of nuclear factor E2-related factor 2 (Nrf2) signaling pathway.

Approximately 15% of all human cancers are estimated to be associated with chronic inflammation and infection [49], with one of the best examples being HCC [50]. Gamma-glutamyl transpeptidase (GGT), a membrane-bound enzyme, exhibits tissue-specific expression which is modified under various physiologic and pathologic conditions, such as development of carcinogenesis [51,52]. GGT activity in the sera of HCC patients has been confirmed as a useful specific HCC marker and its analysis may improve HCC diagnosis [53]. The process of chronic inflammation leads to a stressful microenvironment causing the release of heat shock proteins (HSPs), predominantly, HSP70 and HSP90 [54], and links between the expressions of these HSPs and the oncogenic potential of tumor cells make them likely targets for therapeutic intervention or chemoprevention [55]. Cyclooxygenase-2 (COX-2), another key player in the inflammatory pathway, is overexpressed in chronic liver inflammation, cirrhosis as well as experimental and human HCC [56] and represents a viable target for possible chemopreventive point of attack against inflammation-driven HCC. The eukaryotic transcription factor nuclear factor-kappaB (NF-κB), controller of most genes involved in cell proliferation, adhesion, and inflammatory responses, has been shown to act as a mediator between inflammation and cancer [57,58], making it possible to prevent and treat cancers linked to chronic inflammatory diseases by suppressing the NF-κB-regulated proinflammatory pathways [59].

Our current study aims to understand, identify, and measure the chemopreventive anti-inflammatory mechanisms of dietary BCSE through investigation of the various preneoplastic and proinflammatory markers of hepatocarcinogenesis, namely GGT, HSP70, HSP90, COX-2, and NF-κB. The safety profile of chemopreventive doses of BCSE with special attention to cardiac functions has also been investigated.

MATERIALS AND METHODS

Materials

BCSE was obtained as a dark pink colored powder by the aqueous extraction of the skin of the

black currant fruit followed by spray drying. The detailed extraction procedure and reverse-phase high performance liquid chromatography (RP-HPLC) characterization has been published in our earlier communication [41]. The RP-HPLC analysis indicated that anthocyanins represent approximately 1.2% of the extract, with cyanidin-3-*O*-rutinoside (Figure 1) identified to be the predominant anthocyanin [41]. RNeasy plus mini kit was purchased from Qiagen (Valencia, CA) and superscript II complementary DNA synthesis kit was procured from Invitrogen (Carlsbad, CA). DENA, PB, 2-thiobarbituric acid (TBA), and trichloroacetic acid (TCA) were purchased from Sigma–Aldrich (St. Louis, MO). Pierce BCA kits from Thermo Scientific (Rockford, IL) kits were used for total protein estimation assay. Primary antibodies including rabbit polyclonal HSP70, rabbit polyclonal HSP90, rabbit polyclonal COX-2, rabbit polyclonal NF-κB, and mouse monoclonal β-actin antibody and ABC staining system were obtained from Santa Cruz Biotechnology (Santa Cruz, CA). The horse radish peroxidase (HRP)-conjugated secondary antirabbit and antimouse antibodies used were purchased from Bio-Rad Laboratories (Hercules, CA) and Santa Cruz Biotechnology, respectively. Blocking solution (GE Healthcare) was purchased from GE Healthcare (Little Chalfont, Buckinghamshire, UK) and enhanced chemiluminescence detection kit was obtained from Thermo Scientific. Fast blue BB base solution, cupric sulfate and L-glutamic acid gamma-(4-methoxy-B-naphthylamide) (GMNA) were procured from Sigma–Aldrich while glycylglycine was purchased from Alfa Aesar (Ward Hill, MA).

Experimental Regimen and Liver Harvesting

Liver samples, used for all assays in this study, were harvested from our earlier chemopreventive study [47]. In short, male Sprague–Dawley rats initially weighing about 50–70 g were obtained from Harlan Laboratories (Indianapolis, IN). In accordance with the animal protocol approved and established by the Institutional Animal Care and Use Committee of the Northeast Ohio Medical University, the rats after an acclimatization period of 1 wk were randomly divided into five groups with 6–12 animals/group. Group A serving as normal control and group B as carcinogen control were maintained on a well-defined pulverized basal diet (LabDiet, St. Louis, MO). Animals belonging to groups C, D, and E were subjected to basal diet mixed with various levels of BCSE resulting in two distinct dietary doses for the entire period of the study (22 wk). For group C, 0.125% (w/w) dietary BCSE yielded a dose of 100 mg/kg based on average food intake, whereas 0.625% (w/w) BCSE resulted in a dose of 500 mg/kg for groups D and E (BCSE control). These doses were selected based on a previous rat study with comparable doses that did not show any alteration of hepatic function [60]. After 4 wk of the aforementioned dietary treatment, hepatocarcinogenesis was induced in groups B, C and D by a single intraperitoneal (i.p.) injection of DENA (200 mg/kg). PB, a known tumor promoter [61] was subsequently administered after a period of 2 wk through drinking water at a concentration of 0.05% (w/v). This continued until 4 d prior to the end of the study which concluded at week 22 (18 wk following the DENA administration). All animals were anesthetized, livers were perfused and harvested, and subsequently utilized for analysis of hepatocyte nodules. All data corresponding to the incidence and multiplicity of nodules have been published with the analysis conclusively demonstrating a 15–48% decrease in nodule incidence and 11% and 33% decrease in nodule multiplicity in groups C and D, respectively [47]. Liver samples from various rat groups were immediately flash-frozen in liquid nitrogen, subsequently transferred to and stored at −70°C, and used for various assays as described below.

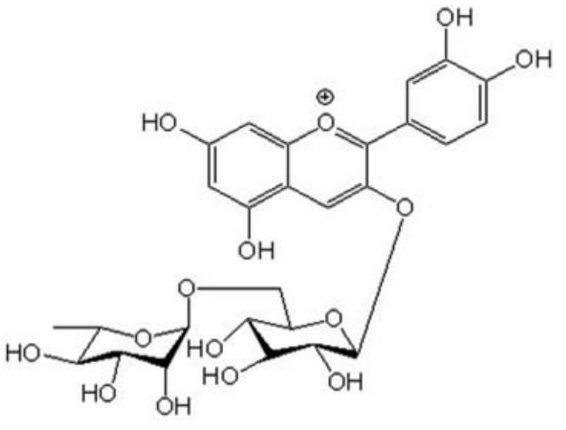

Figure 1. Structure of cyaniding-3-*O*-rutinoside, the predominant anthocyanin present in black currant skin extract.

GGT Assay

GGT expression was studied cytochemically by the modified technique we described recently [62]. In short, hepatic tissue sections (~15 μm) were initially air dried for 30 min, alternating between hot and cold (10 min cycles). The slides were then incubated, at 25°C for 30–45 min in the dark in a freshly prepared and filtered solution of GMNA (125 μg/mL), glycylglycine (500 μg/mL), fast blue BB base solution (500 μg/mL) in tris-buffered saline (0.1 M, pH 7.4). Following incubation, the sections were then washed with 0.85% saline for 2 min and subsequently transferred to a 0.1 M cupric sulfate for 5 min. The sections were washed again in saline solution for 2 min and rinsed with deionized water. The sections were then dried,

counterstained with heamatoxylin and mounted using DPX (Electron Microscopy Sciences, Hatfield, PA). Finally, images of the GGT positive foci were visualized using a light microscope. Four sections from each liver were examined for quantitative evaluation of GGT-positive foci. GGT-positive lesions with more than 0.2 mm in diameter were counted.

Immunohistochemical Assays

Serial sections of liver tissue were used for immunohistochemical analysis of HSP70, HSP90, COX-2, IκB, and NF-κB protein expressions. Frozen sections were first thawed and subsequently air dried, as described above, and the sections were then subjected to antigen retrieval by submersion in 10 mM sodium citrate buffer (pH 6.0) heated up to 80°C for a 10 min time period. The sections were washed for 5 min with PBS and the endogenous peroxidases were blocked by 1% H_2O_2 for 5 min. Blocking solution (5% normal goat serum in PBS) was used for 1 h followed by washing with PBS and incubation with each primary antibody (1:100) overnight at 4°C. Appropriate washing and a 30-min application of HRP-conjugated goat antirabbit secondary antibody (1:200) or HRP-conjugated goat antimouse secondary antibody (1:200) was performed at room temperature and 3,3′-diaminobenzidine tetrahydrocholoride solution was used to develop the chromogenic reaction. After repeated washing three times ranging from 1 to 2 min in 95% and 100% ethanol as well as xylene, sections were finally air dried and mounted using DPX. The immunohistochemical slides were visualized using a light microscope with at least 1000 hepatocytes/animal were analyzed. Results were expressed as percentage of positive cells.

Western Blot Analysis

Frozen liver tissue samples weighing 0.2–0.5 mg were first homogenized in ice-cold lysis buffer to yield a 10% w/v tissue homogenate. The sample was then centrifuged at 4°C at 14 000*g* for 20 min. The supernatant was collected in a separate Eppendorf tube and the pellet was discarded. Total protein content in each sample was quantified using the Pierce BCA protein assay kit. Based on the total protein content, 60 μg of protein sample was loaded per well and run at a constant voltage on a 10% Tris-HCl gel (Bio-Rad Laboratories). The protein, after transfer onto a PVDF membrane, was blocked using 2% Amersham blocking solution for 1 h. Subsequently, primary antibody rabbit polyclonal anti-HSP70 antibody (1:50), rabbit polyclonal anti-HSP90 antibody (1:500), or rabbit polyclonal anti-COX-2 antibody (1:100), rabbit polyclonal anti-IκB antibody (1:100) or rabbit polyclonal anti-NF-κB antibody (1:100) was then applied to the membrane overnight at 4°C. After adequate washing of blot with TBST solution (TBS with 1% Tween 20), the blot was then subjected to 1 h of treatment of HRP-conjugated antirabbit secondary antibody (1:3000) or antimouse secondary antibody (1:1000). The blot washed appropriately with TBST was then subjected to the ECL detection reagent and protein bands were visualized on a Kodak Digital Science Image Station 440CF analyzer. The PVDF membrane was then washed for 15 min with TBST solution, stripped with Restore Western Blot Stripping Buffer (Thermo Scientific) for a period of 20 min and once again washed with TBST solution for 10 min. 2% Amersham blocking solution was reapplied for 1 h and the loading control mouse monoclonal anti-β-actin antibody (1:1000) was applied overnight at 4°C. Following similar steps after the addition of the other primary antibodies, HRP-conjugated antimouse secondary antibody (1:1000) was applied and each blot was developed with ECL substrate and analyzed using the Kodak analyzer.

Reverse Transcription-Polymerase Chain Reaction (PCR)

In accordance with the manufacturer's protocol, the Quick RNA mini Prep kit (Zymo Research, Irvine, CA) was used to extract total RNA from 20 mg of liver tissue. Complementary DNA (cDNA) was synthesized from 1 μg of total RNA using the verso cDNA synthesis kit (Thermo Fisher Scientific, Waltham, MA). PCR was performed using specific primers for rat NF-κB and glyceraldehyde 3-phosphate dehydrogenase (GAPDH) as follows: NF-κB sense: 5′-GAGCCCATGGAGTTCCAGTA-3′; antisense: 5′-ACTTGGTACCATGGCTGAGG; GAPDH sense: 5′-AGACAGCCGCATCTTCTTGT-3′; and antisense: 5′-TACTCAGCACCAGCATCACC-3′. The PCR products were analyzed by agarose gel electrophoresis and visualized by ethidium bromide staining.

Echocardiographic Assessment for Cardiotoxicity

In vivo heart function was assessed noninvasively using a Vevo 770 system (VisualSonics, Toronto, Canada) equipped with a 710B-075 transducer (20–30 MHz) designed specifically for small animal studies at a frame rate of 40–60 Hz as we previously described [63]. Briefly, animals were anesthetized using 2–2.5% sevoflurane via nose cone and placed in the supine position on a heated platform with electrocardiography (ECG) electrodes to monitor heart and respiration rates. M-mode and 2-D images at the mid-papillary level were obtained from the parasternal short-axis view. Mitral valve (MV) inflow was obtained from apical four chamber view followed by PW Doppler. All measurements were averaged from at least three cardiac cycles. Measurements and calculations were performed using the Vevo 770/3.0 software.

Statistical Analysis

Significant changes between various groups were detected by one-way ANOVA. Post hoc analysis was done by the Student–Neuman–Keuls test while a *P*-value less than 0.05 was taken to be significant. The commercially available statistical and graphical software SigmaStat 3.1 (Systat Software, Inc., San Jose, CA) was used for all statistical analysis.

RESULTS

BCSE Suppresses the Induction of GGT-Positive Foci

GGT-positive hepatic foci were not detected in both normal (control) (Figure 2A) and BCSE-treated control (500 mg/kg) liver sections (figure not shown). However, liver sections from animals subjected to DENA administration displayed varied sizes of foci with positive GGT expression. Liver sections from rats exposed to DENA alone showed the highest numbers as well as largest area of GGT-positive foci (Figure 2B), while both treatment groups with BCSE (100 and 500 mg/kg) (groups C and D, respectively), in comparison, were found to show lower number as well as and smaller GGT-positive focal areas (Figure 2C and D). As summarized in Table 1, treatment with the highest dose of BCSE resulted in significant ($P < 0.01$) attenuation in the numbers and area of GGT-positive hepatic foci when compared to the DENA control (group B).

BCSE Abrogates the Elevated Levels of Inflammatory Stress-Induced HSP70

Figure 3A depicts the immunohistochemical staining of HSP70, a key protein released and expressed in conditions of stress, including inflammation [54]. Both normal (control) (Figure 3A-a) and BCSE (500 mg/kg) control group (figure not shown) showed almost no expression of HSP70. High induction of HSP70 is clearly depicted in the DENA control liver section (Figure 3A-b) whilst both DENA-exposed and BCSE-treated groups (groups C and D) showed decreased HSP70 expression compared to DENA-exposed (group B) rats (Figure 3A-c and d). Immunohistochemical analysis of the data (Figure 3B) indicates significantly ($P < 0.001$) elevated levels of HSP70-positive hepatocytes when compared to the normal group. Though decreases are observed with the first treatment dose of BCSE (100 mg/kg), the highest treatment dose of BCSE (500 mg/kg) significantly ($P < 0.01$) attenuated HSP70-positive cells when compared to the DENA control. In order to confirm our immunohistochemical data, we performed Western blotting analysis using liver samples from the various groups and the representative results are illustrated in Figure 3C. The DENA-challenged group demonstrated significant ($P < 0.001$) upregulation in HSP70 protein levels while, in comparison to the DENA control, the highest treatment group with BCSE (500 mg/kg)

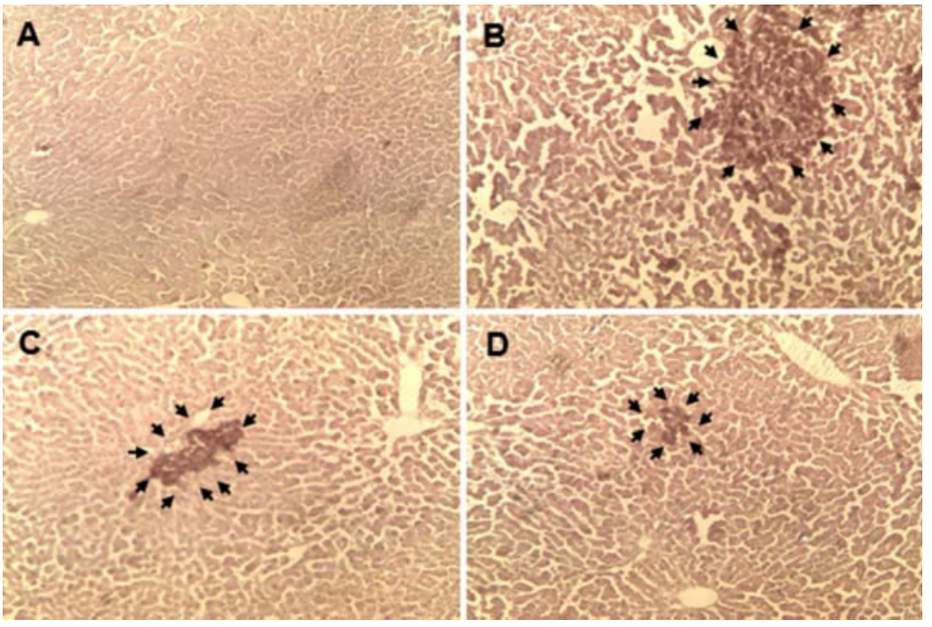

Figure 2. Histochemical detection of hepatic GGT-positive foci in various rat groups (magnification: 100×). Rats were sacrificed 22 wk following the commencement of the study (i.e., 18 wk following DENA exposure). (A) Absence of foci in normal group; (B) a large GGT-positive focus on hepatic section from DENA control rat; (C) a medium size hepatic focus in low dose (100 mg/kg) BCSE + DENA-treated rat; and (D) a small focus in high dose (500 mg/kg) BCSE + DENA-treated rat. GGT-positive foci of various sizes are indicated by arrows. [Color figure can be viewed in the online issue, which is available at wileyonlinelibrary.com]

Table 1. Effects of BCSE on GGT-Positive Hepatic Preneoplastic Foci Induced by DENA in Rats

Groups/treatments	No. of foci/mm^2	Focal area (mm^2/cm^2)
B. DENA control	32.2 ± 1.9	4.02 ± 0.19
C. BCSE (100 mg/kg) + DENA	28.0 ± 3.1	3.55 ± 0.39
D. BCSE (500 mg/kg) + DENA	18.7 ± 0.6*	2.35 ± 0.06*

Animals from normal (Group A) and BCSE (500 mg/kg) control group (Group E) did not show any GGT-positive foci.
Values are presented as means ± SEMs of four animals.
BCSE, black currant skin extract; DENA, diethylnitrosamine; GGT, gamma-glutamyl transpeptidase; SEM, standard error of mean.
*$P < 0.01$ as compared with DENA control (Group B).

displayed a significant ($P < 0.001$) attenuation of the elevated HSP70 expression level.

BCSE Suppresses the Increased Levels of Inflammatory Stress-Induced HSP90

HSP90, a molecular chaperone and predominant HSP has been found to be upregulated in HCC [64,65]. Figure 4A is the representative immunohistochemical profile of HSP90 in several rat groups. Almost no HSP90 protein was expressed in liver sections from the normal (control) group (Figure 4A-a). The same was also true for the BCSE (500 mg/kg) control group (figure not shown). However, as illustrated in Figure 4A-b, immunostaining of liver sections from the DENA-control group showed elevated levels of HSP90 expression, while both BCSE (100 and 500 mg/kg) treatment groups depicted downregulation in HSP90 expression compared to DENA control (Figure 4A-c and d, respectively). Quantitative analysis of the immunohistochemical data (Figure 4B) revealed a significant ($P < 0.001$) elevation in HSP90-positive liver cells in DENA-treated group (group B) when compared to the normal group (Figure 4B). BCSE treatment at both doses decreased these immunopositive cells with the highest dose of BCSE (500 mg/kg) eliciting significant ($P < 0.01$) reduction in HSP90 expression compared to the DENA control. We have also used liver samples from various groups for Western blotting analysis and the results obtained (Figure 4C and D) conformed our immunohistochemical data with the

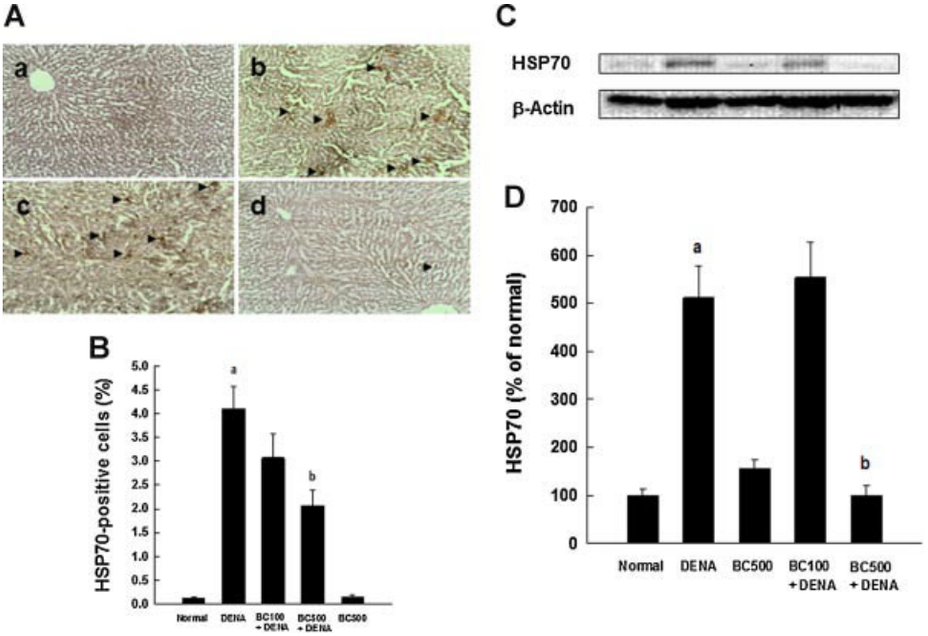

Figure 3. Effects of BCSE on hepatic HSP70 expression during DENA-initiated hepatocarcinogenesis in rats. (A) Representative immunohistochemical localization of HSP70 (magnification: 100×). Arrowheads indicate immunohistochemical staining of HSP70. (B) Quantification of HSP70 positive cells based on 1000 hepatocytes per animal and 4 animals per group. Each bar represents the mean ± SEM ($n = 4$). [a]$P < 0.001$ as compared with normal group; [b]$P < 0.05$ as compared with DENA control. (C) Representative Western blot and (D) densitometric analysis of hepatic HSP70 expression. Each bar represents the mean ± SEM ($n = 4$–6). [a]$P < 0.001$ as compared with normal group; [b]$P < 0.001$ as compared with DENA control. [Color figure can be viewed in the online issue, which is available at wileyonlinelibrary.com]

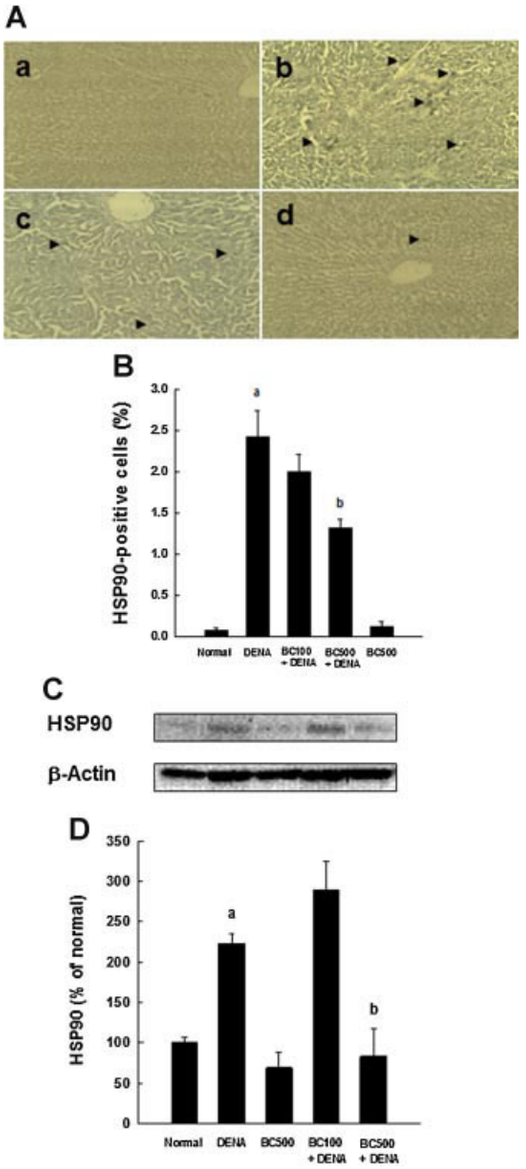

Figure 4. Effects of BCSE on hepatic HSP90 expression during DENA-initiated hepatocarcinogenesis in rats. (A) Representative immunohistochemical localization of HSP90 (magnification: 100×). Arrowheads indicate immunohistochemical staining of HSP90. (B) Quantification of HSP90 positive cells based on 1000 hepatocytes per animal and 4 animals per group. Each bar represents the mean ± SEM ($n = 4$). $^{a}P < 0.001$ as compared with normal group; $^{b}P < 0.05$ as compared with DENA control. (C) Representative Western blot and (D) densitometric analysis of hepatic HSP90 expression. Each bar represents the mean ± SEM ($n = 4$–6). $^{a}P < 0.001$ as compared with normal group; $^{b}P < 0.001$ as compared with DENA control. [Color figure can be viewed in the online issue, which is available at wileyonlinelibrary.com]

DENA-administered control (group B) exhibiting a significant ($P < 0.01$) induction in HSP90 protein level compared to the normal group. In contrast, both BCSE treatment doses (100 and 500 mg/kg) downregulated this elevated expression of HSP90 with respect to the DENA-challenged group alone. Significant ($P < 0.01$) reduction was observed with the highest treatment dose of BCSE (500 mg/kg) (group D) compared to the DENA control (group B).

BCSE Diminishes the Upregulated Levels of COX-2

Undetectable in most normal tissues, COX-2 is heavily induced by the inflammatory cascade as well as being responsible for the increased production of prostaglandins during inflammation [66]. Figure 5A represents the immunohistochemical staining captured with both the normal (control) (Figure 5A-a) and BCSE (500 mg/kg) control (figure not shown) depicting limited or almost no expression of COX-2. In contrast, the DENA-exposed control (Figure 5A-b) indicated a higher frequency of COX-2 positive cells while groups C and D, treated with BCSE (100 and 500 mg/kg respectively) after DENA exposure, appeared to have fewer numbers of COX-2-positive cells. In Figure 5B, immunohistochemical analysis revealed significant ($P < 0.001$) increase in the number of COX-2-positive hepatocytes compared to the normal group, whereas a significantly ($P < 0.001$) lowered expression of COX-2 immunopositivity was observed in the group of animals treated with the highest dose of BCSE (500 mg/kg) (group D). Figure 5C pertains to the Western blot performed for acquiring COX-2 protein expression among the various groups of rats and Figure 5D represents our analysis of the blot which was in agreement with our immunohistochemical analysis. Compared to the normal group, COX-2 protein expression was found to be significantly ($P < 0.001$) induced in the DENA-challenged animals (group B) while the DENA-administered and BCSE-treatment groups (100 and 500 mg/kg) both displayed decreases in COX-2 protein expression. A significant ($P < 0.001$) result was obtained with reference to BCSE (500 mg/kg) treatment group compared to the DENA control.

BCSE Induces NF-κB Expression at Both Transcription and Translation Levels

Touted as the potential link between inflammation and cancer, the ubiquitously expressed NF-κB plays a central role in inflammatory and immune responses [67,68]. Normally sequestered in the cytoplasm by IκB, NF-κB translocates to the nucleus, under inflammatory and other stressful stimuli, to activate expression of many proinflammatory gene [69]. Figure 6A(a–d) depicts the immunohistochemical staining of cytosolic as well as nuclear NF-κB protein whereas Figure 6A(b,c) represents the staining for cytosolic expression of IκBα in liver sections from the various groups. The normal (control) group demonstrates very low expression of NF-κB in the nucleus and moderate expression of the same in the cytosol (Figure 6A-a). DENA control (group B) demonstrates an increase in the

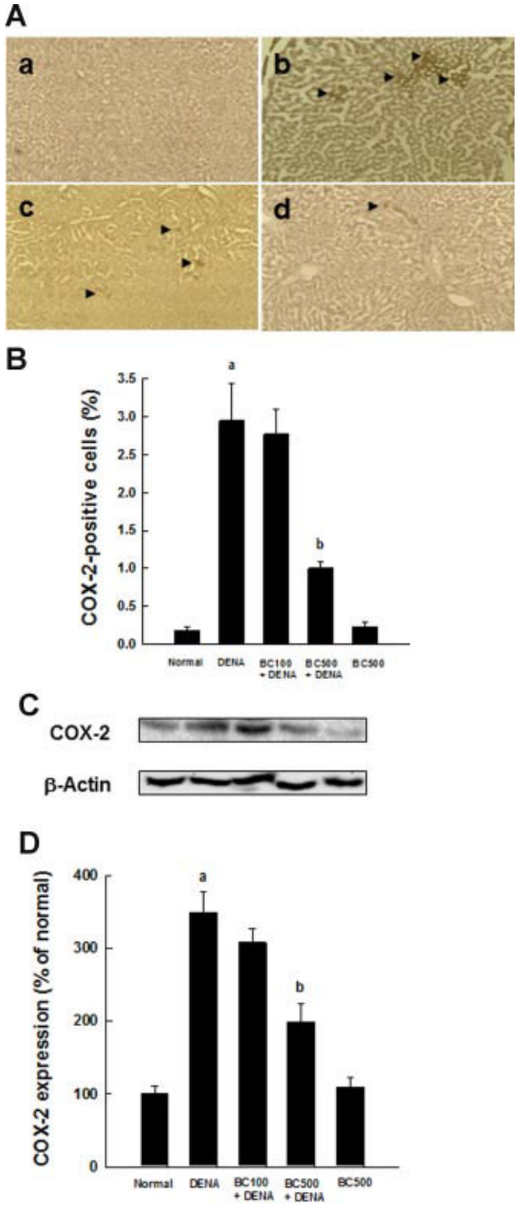

Figure 5. Effects of BCSE on hepatic COX-2 expression during DENA-initiated hepatocarcinogenesis in rats. (A) Representative immunohistochemical localization of COX-2 (magnification: 100×). Arrowheads indicate immunohistochemical staining of COX-2. (B) Quantification of COX-2 positive cells based on 1000 hepatocytes per animal and 4 animals per group. Each bar represents the mean ± SEM ($n = 4$). [a]$P < 0.001$ as compared with normal group; [b]$P < 0.05$ as compared with DENA control. (C) Representative Western blot and (D) densitometric analysis of hepatic COX-2 expression. Each bar represents the mean ± SEM ($n = 4$–6). [a]$P < 0.001$ as compared with normal group; [b]$P < 0.001$ as compared with DENA control. [Color figure can be viewed in the online issue, which is available at wileyonlinelibrary.com]

expression of nuclear NF-κB and almost disappearance of cytosolic NF-κB (Figure 6A-b). The treatment with BCSE at 100 mg/kg shows a slight decrease in the number of immunopositive cells for NF-κB in the nucleus (Figure 6A-c) whereas the highest treatment dose of BCSE (500 mg/kg) clearly indicate a substantial reduction of nuclear NF-κB expression and elevation of cytosolic NF-κB expression indicating limited translocation of NF-κB from the cytosol to the nucleus. An interesting observation was made in terms of cytosolic expression of IκBα: moderate expression in normal (Figure 6A-e), almost no expression in DENA control (Figure 6A-f), limited expression in low dose BCSE group (Figure 6A-g) and substantial expression in high dose BCSE (Figure 6A-h). Figure 6B represents the immunohistochemical analysis of percentage of immunopositive cells. The expression of nuclear p65 is significantly ($P < 0.001$) greater in DENA control than that of the normal group but treatment with BCSE at 500 mg/kg significantly ($P < 0.01$) inhibited the translocation of NF-κB to the nucleus, with less numbers of NF-κB immunopositive cells in nucleus when compared to DENA control. Concurrently, cytosolic expression of NF-κB in DENA control is significantly ($P < 0.01$) lower in comparison to the normal (control), whilst treatment with the highest dose of BCSE (500 mg/kg) significantly ($P < 0.01$) elevated the expression of cytosolic NF-κB. Cytosolic IκBα was significantly ($P < 0.001$) lower in DENA control with respect to the normal group and BCSE treatment at 500 mg/kg showed significant ($P < 0.01$) elevation in the expression of cytosolic IκBα.

Figure 7A represents the Western blot performed to analyze NF-κB p65 protein expression among the liver samples collected from each group. Increased expression this protein in the DENA control animals (group B) and the substantial attenuation of this expression with the treatment of high dose BCSE (500 mg/kg) demonstrates the results to be in conformation with that of our immunohistochemical data. To further substantiate our Western blot analysis, RT-PCR was conducted to determine the mRNA levels of NF-κB p65. There is an increase in the gene expression of NF-κB p65 in the DENA-challenged control versus that of the normal and the treatment BCSE (at 500 mg/kg) showing a dramatic decrease in NF-κB p65 gene expression as compared to DENA control.

BCSE Does Not Affect Cardiac Function, Remodeling, or Mitral Valve Blood Flow

Echocardiography was performed at the end of the treatment period just prior to sacrifice to assess the effects of BCSE on cardiac performance. None of the key parameters for cardiac function (ejection fraction, fractional shortening), cardiac dimensions or remodeling (left ventricular volume or mass), or blood flow (mitral valve E/A ratio) were significantly different across the experimental

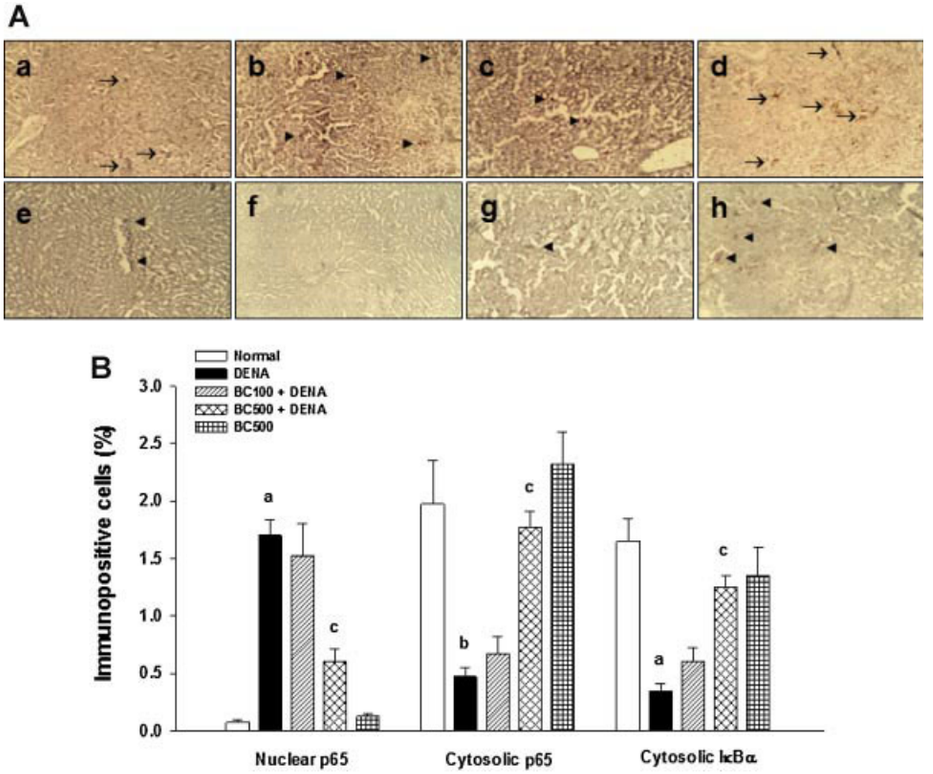

Figure 6. Effects of BCSE on hepatic NF-κB p65 translocation and inhibitor of κB (IκB-α) degradation during DENA-evoked hepatic preneoplasia in Sprague-Dawley rats. (A) Representative immunohistochemical localization of NF-κB p65 in nucleus (b and c; arrowheads) and cytosol (a and d; arrows) and IκB-α in cytosol (e–h) (magnification: 100×). Rats were sacrificed 22 wk following the commencement of the study and immunohistochemistry was performed to detect NF-κB p65 as well as IκB-α. Arrows indicate immunohistochemical staining. Different experimental groups are: (a) and (e) normal control; (b) and (f) DENA control; (c) and (g) BCSE 100 mg/kg + DENA; and (d) and (h) BCSE 500 mg/kg + DENA. (B) Quantification of NF-κB p65- and IκB-α-immunopositive cells in rat livers of several experimental groups. One thousand hepatocytes were counted per animal and the results were based on 4 animals per group. Each bar represents the mean ± SEM ($n = 4$). $^{a}P < 0.001$ and $^{b}P < 0.01$ as compared to normal group; $^{c}P < 0.01$ as compared to DENA control. [Color figure can be viewed in the online issue, which is available at wileyonlinelibrary.com]

groups (Table 2) indicating that BCSE treatments, at both dose levels, were noncardiotoxic under the experimental conditions of the present study.

DISCUSSION

Our previous studies [47,48] have identified BCSE to be an efficacious chemopreventive agent against DENA-induced hepatocarcinogenesis by virtue of its Nrf2-mediated antioxidant mechanisms. The link between inflammation and cancer has been hypothesized over a century ago by Rudolf Virchow [70]. Approximately 20% of all cancer deaths have been estimated to be associated with chronic infections and recurring inflammation [71] with HCC being one primary example [72]. In the light of such knowledge, suppression of the inflammatory cascade represents a key target of chemoprevention to halt the progress of preneoplastic lesions into a full-blown state of hepatic neoplasia. Our present study, therefore, was designed to identify if BCSE was capable to suppress NF-κB-mediated inflammatory pathways including the inflammation-driven expression of HSP70, HSP90 as well as COX-2 during an early event of rat liver carcinogenesis.

GGT, a widely distributed hepatospecific enzyme, is used as a marker of biochemical alteration in hepatocellular foci, nodules and tumor in rats [53,73]. GGT-induction in preneoplastic foci is considered an early event in HCC occurrence while GGT-positive foci are regarded as the first evidence of the tumor initiation process [73]. Immunohistochemical detection and analysis of GGT-positive foci have lately been established and widely used as quantitative methods to detect any modulatory effects exerted by dietary agents against the hepatocarcinogenic progress [62]. Our results have elucidated the effects of dietary BCSE to significantly reduce the number and size of GGT-positive focal areas, indicating chemopreventive activities during both the initiation as well as

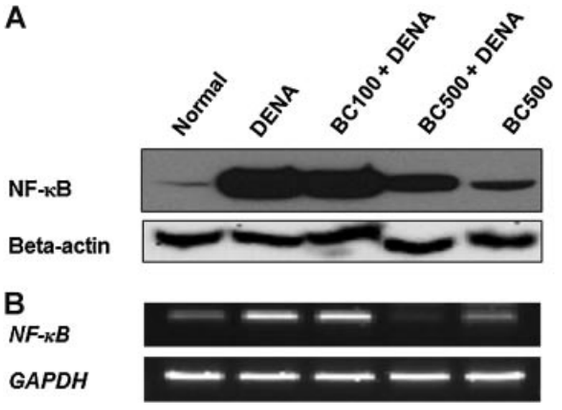

Figure 7. Effects of BCSE on hepatic NF-κB p65 expression in DENA-initiated hepatocarcinogenesis in rats. (A) Representative Western blot analysis of NF-κB p65 subunit. Total protein was separated and blotted with anti-NF-κB p65 antibody. The blots were stripped and reprobed with anti-β-actin antibody to ensure the loading of equal amount of protein. (B) Representative RT-PCR analysis of hepatic NF-κB p65 expression in various groups of rats. Total hepatic RNA was isolated, subjected to reverse transcription, and resulting cDNA was subjected to RT-PCR analysis using specific primer sequence. The *GAPDH* was used as the housekeeping gene.

promotional stages of DENA-induced hepatocarcinogenesis in rats.

HSPs are a ubiquitous and highly conserved group of molecules which usually function as defense mechanisms for protecting cells from various environmental stresses [74,75]. HSPs are divided into six families, namely HSP100, HSP90, HSP70, HSP60, HSP40, and small HSPs including HSP27 [76–79]. HSP70 is often overexpressed in various malignant cells and have been suggested to contribute to hepatocarcinogenesis and hepatic tumor progression by promoting tumor cell proliferation [54,80,81]. HSP90 modulates the expression and function of many known hepatocarcinogenic factors, and its upregulation in concurrence with cyclin-dependent kinase 4 (CDK4) activity has been shown to contribute to HCC development [82–85]. The inhibition of HSP90 induces the simultaneous degradation and inactivation of hepatocarcinogenesis-driving factors as well as cell cycle arrest and apoptosis in HCC cells [86]. Targeting HSPs by inhibiting their expression could lead to the potential reduction in inflammatory stress and therefore an ideal method to curb the occurrence of HCC. Our current study utilized both Western blotting as well as immunohistochemical techniques to demonstrate elevated levels of both HSP70 and HSP90 expression in DENA-exposed rats which are in agreement with other studies [87,88]. Upon continuous treatment with dietary BCSE, these overexpressed protein levels of HSP70 and HSP90 were significantly suppressed indicating a definite attenuation of the inflammation-mediated hepatocarcinogenic stress generated by DENA.

COX-2, the inducible enzyme responsible for catalyzing the conversion of arachidonic acid to prostaglandins (PGs), has been suggested to play a significant role in inflammation-related hepatocarcinogenesis [89]. Over-expression of COX-2 in tumors leads to an increase in PG levels which affect multiple mechanisms involved in carcinogenesis, such as angiogenesis, inhibition of apoptosis, and stimulation of cell growth along with invasiveness and metastatic potential of tumor cells [90]. Several studies have shown selective COX-2 inhibition suppresses proliferation of HCC cells [91–95] as well as prevent hepatocarcinogenesis in rodents [96]. From a chemopreventive approach, inhibiting COX-2 appears as an exciting and viable strategy, especially using dietary agents that confer no toxicity upon consumption. In concurrence to other studies [91,97], our results demonstrated elevated hepatic expressions of COX-2 in the rats subjected

Table 2. Doppler Echocardiographic Parameters of Various Rat Groups at the End of the Study

Parameters	Normal	DENA control	BCSE (500 mg/kg) control	BCSE (100 mg/kg) + DENA	BCSE (500 mg/kg) + DENA
Ejection fraction (%)	72.73 ± 0.89	73.19 ± 2.51	70.40 ± 2.37	66.60 ± 1.91	68.51 ± 1.79
Fractional shortening (%)	43.26 ± 0.86	44.02 ± 2.20	41.46 ± ± 2.00	38.40 ± 1.58	39.81 ± 1.49
LV volume (diastolic) (μL)	313.3256 ± 20.39	341.30 ± 14.23	323.42 ± 13.40	343.06 ± 14.31	331.12 ± 24.59
LV mass (corrected) (mg)	969.85 ± 27.84	920.93 ± 53.86	907.17 ± 35.92	959.13 ± 35.91	839.55 ± 8.94
Mitral valve E/A ratio	1.08 ± 0.03	1.00 ± 0.07	1.08 ± 0.04	1.02 ± 0.03	1.05 ± 0.08

Values are presented as means ± SDs of five animals.
BCSE, black currant skin extract; DENA, diethylnitrosamine; E/A ratio, mitral valve early to late atrial flow ratio; LV, left ventricular; SD, standard deviation.

to DENA alone while BCSE treatment dose-dependently revoked these upregulated levels of COX-2, thereby indicating anti-inflammatory mechanisms. As opposed to many synthetic COX-2 inhibitors, BCSE-mediated inhibition of COX-2 has been achieved without any cardiotoxicity which represents a novel finding of the current investigation. This is in agreement with prior studies indicating the beneficial effects of black currant consumption on the cardiovascular system. The ability of black currants to decrease the risk of cardiovascular incidents has been linked to vaso-relaxation through endothelial histamine H_1 receptors, indirectly increasing nitric oxide levels [98]. Another study demonstrated a reduction of peripheral vascular resistance by black currant concentrate in a rat hind-limb perfusion model [99]. Human consumption of black currant juice demonstrated an improvement in the attenuation of serum cholesterol by macrophages by increasing the expression of paraoxanase 1 which is a major antiatherosclerotic component of high-density lipoprotein [100]. Interestingly, our previous study showed that the highest dose of BCSE (500 mg/kg) did not produce any adverse effects including hepatotoxicity based on histopathological assessment [47].

Studied extensively in rodent models of hepatocarcinogenesis, the eukaryotic transcription factor NF-κB is a major driving force in the expression of many inflammatory cytokines, adhesion molecules, angiogenic factors, and enzymes like COX-2 and iNOS which constitute as important molecules required for the synthesis of inflammatory mediators namely prostaglandin E2 and nitric oxide. When exposed to carcinogens, NF-κB promotes cell survival and proliferation through the activation of genes encoding for proteins involved in the antiapoptotic pathway and cell cycle progression [101]. NF-κB consists of dimers assembled from two of five subunits—p65 (RelA), c-Rel, RelB, p50/NF-κB1, and p52/NF-κB2 [102]. Under normal conditions, NF-κB dimers are bound to specific inhibitory proteins including IκB in the cytoplasm. The NF-κB classical signaling pathway can be activated by proinflammatory signals and other stimuli, mainly through IκB kinase (IKK)-dependent phosphorylation and degradation of the IκB inhibitory proteins. The IKK-dependent phosphorylation of IκBs marks them for ubiquitination and subsequent degradation. NF-κB is now free of IκB which now translocates to the nucleus, where it activates the transcription of target genes, including cytokines and antiapoptotic factors [69]. Following its translocation to the nucleus, NF-κB is able to induce the transcription of specific genes including COX-2, whose promoter region has binding sites for NF-κB, which has been well implicated in the hepatocarcinogenic progress [56,103–105] In the current study, we measured the expressions of the p65 subunit of NF-κB in both the hepatic nuclear and cytosolic compartments as well as IκB protein expression in the cytosol. Our study reports that in the DENA-control rodents, the expression of IκB in the cytosol was minimal, owing to degradation, while NF-κB p65 expression in the nucleus was higher corresponding to its translocation to the nucleus due to the inflammatory stimuli instigated by DENA exposure. DENA-induced inflammation triggered reactive oxygen species (ROS) production which subsequently activates NF-κB signaling, followed by the release of chemokines, iNOS, and other proinflammatory cytokines; all these contributing as events that ultimately result in hepatocarcinogenesis [106]. With its ability to decrease the degradation of IκB and halt translocation of p65 to the nucleus, it can be inferred that BCSE can suppress DENA-initiated NF-κB signaling and therefore inhibits the downstream inflammatory cascade.

The results of our present investigation together with the results from other laboratories indicate that anthocyanins present in BCSE may confer, at least in part, the observed anti-inflammatory effect of black currants during rat liver tumorigenesis. Black currant fruits are known to contain the highest level of anthocyanins, superseding the amount present in other prominent sources, such as blackberries and blueberries [107]. Nevertheless, there exists the possibility that other bioactive constituents we have recently identified in the BCSE, such as ferulic acid, sitosterin, and gallic acid (unpublished observation) may contribute to inflammation suppressing effect of BCSE used in the current study. The highest dose of BCSE (500 mg/kg) used in our study is equivalent to rat consumption of 200 g fresh black currant fruit/kg body weight. Hence, the chemopreventive doses of BCSE in the present study may be considered to be high and cannot be directly correlated with the extent of black currant consumption by humans to yield similar benefits. While more studies are needed to understand the full translational impact of the current study, it is possible that black currant phytoconstituents can be provided as safe daily supplements in humans, especially those who are at a high risk of developing HCC. Interestingly, a recently concluded clinical study reported that short-term consumption of concentrated freeze-dried whole black currant fruit extract (equivalent to 48 g fruit) exhibited antioxidant and anti-inflammatory properties [37]. The dose of the hepatocarcinogen (DENA) used in our study is substantially greater than known dietary levels of carcinogens [108]. In this background, if black currant phytochemicals could efficiently inhibit liver tumor formation in rats, then low exposure to dietary black currant could also be effective against comparably lower exposures to carcinogens in humans.

Collectively, the results of our current investigation convincingly demonstrate that BCSE is capable of abrogating DENA-mediated early hepatocarcinogenesis by suppressing the inflammatory cascade characterized by the reversal of the overexpression of HSP70, HSP90, and COX-2 as well as blockade of the nuclear translocation of NF-κB. Our laboratory has previously documented the chemopreventive effects of BCSE against DENA-induced hepatocarcinogenesis [47] as well as the involvement of antioxidant mechanism of action [48]. Hence, the results of our present findings in conjunction with previously reported results establish antioxidative and anti-inflammatory properties as the underlying mechanisms of the powerful chemopreventive activities of black currant phytochemicals. These extraordinary properties coupled with an excellent safety profile, we believe, can lend hope toward the potential utilization of black currants and/or their bioactive constituents in preventing the so-far incurable neoplastic disease of the liver.

ACKNOWLEDGMENTS

A part of this work was carried out at the Northeast Ohio Medical University (Rootstown, OH) supported by a start-up research grant to A.B. We thank Rajiv Lotey and Thomas Mbimba for assistance with animal feeding and tissue harvesting, Kendra F. Barnes for analytical work, and Danielle M. Petit and Karishma A. Samtani for immunohistochemical studies.

REFERENCES

1. World Health Organization. The global burden of disease: 2004 update. Geneva: World Health Organization; 2008.
2. Jemal A, Bray F, Center MM, Ferlay J, Ward E, Forman D. Global cancer statistics. CA Cancer J Clin 2011;61: 69–90.
3. Perz JF, Armstrong GL, Farrington LA, Hutin YJ, Bell BP. The contributions of hepatitis B virus and hepatitis C virus infections to cirrhosis and primary liver cancer worldwide. J Hepatol 2006;45:529–538.
4. El-Serag HB, Rudolph KL. Hepatocellular carcinoma: Epidemiology and molecular carcinogenesis. Gastroenterology 2007;132:2557–2576.
5. Bosetti C, Levi F, Boffetta P, Lucchini F, Negri E, La Vecchia C. Trends in mortality from hepatocellular carcinoma in Europe, 1980–2004. Hepatology 2008;48:137–145.
6. Altekruse SF, McGlynn KA, Reichman ME. Hepatocellular carcinoma incidence, mortality, and survival trends in the United States from 1975 to 2005. J Clin Oncol 2009;27:1485–1491.
7. El-Serag HB. Hepatocellular carcinoma: Recent trends in the United States. Gastroenterology 2004;127:S27–S34.
8. Bartsch H, Montesano R. Relevance of nitrosamines to human cancer. Carcinogenesis 1984;5:1381–1393.
9. Kensler TW, Egner PA, Wang JB, et al. Chemoprevention of hepatocellular carcinoma in aflatoxin endemic areas. Gastroenterology 2004;127:310–318.
10. Schütte K, Bornschein J, Malfertheiner P. Hepatocellular carcinoma—Epidemiological trends and risk factors. Dig Dis 2009;27:80–92.
11. Pircher A, Medinger M, Drevs J. Liver cancer: Targeted future options. World J Hepatol 2011;3:38–44.
12. Rossi L, Zoratto F, Papa A, et al. Current approaches in the treatment of hepatocellular carcinoma. World J Gastrointest Oncol 2010;2:348–359.
13. Sporn MB, Suh N. Chemoprevention of cancer. Carcinogenesis 2000;3:525–530.
14. Jordan VC. Chemoprevention of breast cancer with selective oestrogen-receptor modulators. Nat Rev Cancer 2007;1:46–53.
15. Castrellon AB, Glück S. Chemoprevention of breast cancer. Expert Rev Anticancer Ther 2008;8:443–452.
16. Bishayee A, Politis T, Darvesh AS. Resveratrol in the chemoprevention and treatment of hepatocellular carcinoma. Cancer Treat Rev 2010;36:43–53.
17. Seeram NP. Berries. In: Heber D, Blackburn G, Go V, Milner J, editors. Nutritional oncology. Amsterdam: Elsevier, Inc.; 2006. pp. 615–628.
18. Alwerdt JL, Seigler DS, Gonzalez de Mejia E, Yousef GG, Lila MA. Influence of alternative liquid chromatography techniques on the chemical complexity and bioactivity of isolated proanthocyanidin mixtures. J Agric Food Chem 2008;56:1896–1906.
19. Szajdek A, Borowska EJ. Bioactive compounds and health-promoting properties of berry fruits: A review. Plant Foods Hum Nutr 2008;63:147–156.
20. Nurmi T, Mursu J, Heinonen M, Nurmi A, Hiltunen R, Voutilainen S. Metabolism of berry anthocyanins to phenolic acids in humans. J Agric Food Chem 2009;57: 2274–22781.
21. Stoner GD, Wang LS, Casto BC. Laboratory and clinical studies of cancer chemoprevention by antioxidants in berries. Carcinogenesis 2008;29:1665–1667.
22. Seeram NP. Recent trends and advances in berry health benefits research. J Agric Food Chem 2010;58:3869–3870.
23. Seeram NP, Stoner GD. Berries and cancer prevention. New York: Springer; 2011.
24. Declume C. Anti-inflammatory evaluation of a hydroalcoholic extract of black currant leaves (*Ribes nigrum*). J Ethnopharmacol 1989;27:91–98.
25. Nielsen IL, Haren GR, Magnussen EL, Dragsted LO, Rasmussen SE. Quantification of anthocyanins in commercial black currant juices by simple high-performance liquid chromatography. Investigation of their pH stability and antioxidative potency. J Agric Food Chem 2003;51: 5861–5866.
26. Wu X, Gu L, Prior RL, McKay S. Characterization of anthocyanins and proanthocyanins in some cultivars of *Ribes*, *Aronia*, and *Sambucus* and their antioxidant capacity. J Agric Food Chem 2004;52:7846–7856.
27. Scalzo J, Currie A, Stephens J, McGhie T, Alspach P. The anthocyanin composition of different *Vaccinium*, *Ribes* and *Rubus* genotypes. Biofactors 2008;34:13–21.
28. Paredes-López O, Cervantes-Ceja ML, Vigna-Pérez M, Hernández-Pérez T. Berries: Improving human health and healthy aging, and promoting quality life—A review. Plant Foods Hum Nutr 2010;65:299–308.
29. Clifford MN. Anthocyanins—Nature, occurrence and dietary burden. J Sci Food Agric 2000;80:1063–1072.
30. Lister CE, Wilson PE, Sutton KH, Morrison SC. Understanding the health benefits of blackcurrants. Proc 8th Int *Rubus ribes* Symp 2002;1–2:443–449.
31. Amakura Y, Umino Y, Tsuji S, Tonogai Y. Influence of jam processing on the radical scavenging activity and phenolic content in berries. J Agric Food Chem 2000;48:6292–6297.
32. Hertog MGL, Feskens EJM, Hollman PCH, Katan MB, Kromhout D. Dietary antioxidant flavonoids and risk of coronary heart disease: The Zutphen elderly study. Lancet 1993;342:1007–1011.

33. Garbacki N, Tits M, Angenot L, Damas J. Inhibitory effects of proanthocyanidins from *Ribes nigrum* leaves on carrageenin acute inflammatory reactions induced in rats. BMC Pharmacol 2004;4:25; PMID: 15498105.
34. Garbacki N, Kinet M, Nusgens B, Desmecht D, Damas J. Proanthocyanidins, from *Ribes nigrum* leaves, reduce endothelial adhesion molecules ICAM-1 and VCAM-1. J Inflamm 2005;2:9; PMID: 16091140.
35. Puupponen-Pimia R, Nohynek L, Meier C, et al. Antimicrobial properties of phenolic compounds from berries. J Appl Microbiol 2001;90:494–507.
36. Hurst SM, McGhie TK, Cooney JM, et al. Blackcurrant proanthocyanidins augment IFN-gamma-induced suppression of IL-4 stimulated CCL26 secretion in alveolar epithelial cells. Mol Nutr Food Res 2010;54:1–12.
37. Lyall KA, Hurst SM, Cooney J, et al. Short-term blackcurrant extract consumption modulates exercise-induced oxidative stress and lipopolysaccharide-stimulated inflammatory responses. Am J Physiol Reg Integr Comp Physiol 2009;297:R70–R78.
38. Olsson M, Gustavsson KE, Andersson S, Nilsson Å, Duan RD. Inhibition of cancer cell proliferation in vitro by fruit and berry extracts and correlations with antioxidant levels. J Agric Food Chem 2004;52:7264–7271.
39. Boivin D, Blanchette M, Barrette S, Moghrabi A, Béliveau R. Inhibition of cancer cell proliferation and suppression of TNF-induced activation of NF-κB by edible berry juice. Anticancer Res 2007;27:937–948.
40. McDougall GJ, Ross HA, Ikeji M, Stewart D. Berry extracts exert different antiproliferative effects against cervical and colon cancer cells grown in vitro. J Agric Food Chem 2008;56:3016–3023.
41. Bishayee A, Háznagy-Radnai E, Mbimba T, et al. Anthocyanin-rich black currant extract suppresses the growth of human hepatocellular carcinoma cells. Nat Prod Commun 2010;5:1613–1618.
42. Jo JY, de Mejia EG, Lila MA. Cytotoxicity of bioactive polymeric fractions from grape cell culture on human hepatocellular carcinoma, murine leukemia and noncancerous PK15 kidney cells. Food Chem Toxicol 2006; 44:1758–1767.
43. Yeh CT, Yen GC. Induction of apoptosis by anthocyanidins through regulation of Bcl-2 gene and activation of c-jun N-terminal kinase cascade in hepatoma cells. J Agric Food Chem 2005;53:1740–1749.
44. Shin DY, Ryu CH, Lee WS, et al. Induction of apoptosis and inhibition of invasion in human hepatoma cells by anthocyanidins from Meoru. Ann NY Acad Sci 2009; 1171:137–148.
45. Takata R, Yamamoto R, Yanai T, Konno T, Okubo T. Immunostimulatory effects of a polysaccharide-rich substance with antitumor activity isolated from black currant (*Ribes nigrum* L.). Biosci Biotechnol Biochem 2005;69: 2042–2050.
46. Takata R, Yanai T, Yamamoto R, Konno T. Improvement of the antitumor activity of black currant polysaccharide by an enzymatic treatment. Biosci Biotechnol Biochem 2007;71:1342–1344.
47. Bishayee A, Mbimba T, Thoppil RJ, et al. Anthocyanin-rich black currant (*Ribes nigrum* L.) extract affords chemoprevention against diethylnitrosamine-induced hepatocellular carcinogenesis in rats. J Nutr Biochem 2011; 22:1035–1046.
48. Thoppil RJ, Bhatia D, Barnes KF, et al. Black currant anthocyanins abrogate oxidative stress through Nrf2-mediated antioxidant mechanisms in a rat model of hepatocellular carcinoma. Curr Cancer Drug Targets 2012; in press.
49. Schafer M, Werner S. Cancer as an overhealing wound: An old hypothesis revisited. Nat Rev Mol Cell Biol 2008;9:628–638.
50. Seeff LB. Introduction: The burden of hepatocellular carcinoma. Gastroenterology 2004;127:S1–S4.
51. Tang QY, Yao DF, Lu JX, Wu XH, Meng XY. Expression and alterations of different molecular form gammaglutamyl transferase and total RNA concentration during the carcinogenesis of rat hepatoma. World J Gastroenterol 1999;5:356–358.
52. Yao DF, Dong ZZ, Yao DB, et al. Abnormal expression of hepatoma-derived gammaglutamyltransferase subtyping and its early alteration for carcinogenesis of hepatocytes. Hepatobiliary Pancreat Dis Int 2004;3:564–570.
53. Yao DF, Huang ZW, Chen SZ, et al. Diagnosis of hepatocellular carcinoma by quantitative detection of hepatoma-specific bands of serum gamma-glutamyltransferase. Am J Clin Pathol 1998;110:743–749.
54. Joo M, Chi JG, Hyucksang L. Expressions of HSP70 and HSP27 in hepatocellular carcinoma. J Korean Med Sci 2005;20:829–834.
55. Murakami A, Ashida H, Terao J. Multitargeted cancer prevention by quercetin. Cancer Lett 2008;269:315–325.
56. Wu T. Cyclooxygenase-2 in hepatocellular carcinoma. Cancer Treat Rev 2006;32:28–44.
57. Karin M. The IκB kinase-a bridge between inflammation and cancer. Cell Res 2008;18:334–432.
58. Muriel P. NF-κB in liver diseases: A target for drug therapy. J Appl Toxicol 2009;29:91–100.
59. Aggarwal BB, Vijayalekshmi RV, Sung B. Targeting inflammatory pathways for prevention and therapy of cancer: Short-term friend, long-term foe. Clin Cancer Res 2009;15:425–430.
60. Frank J, Kamal-Eldin A, Lundh T, Maaatta K, Torronen R, Vessby B. Effects of dietary anthocyanins on tocopherols and lipids in rats. J Agric Food Chem 2002;50:7226–7230.
61. Lans M, de Gerlache J, Taper HS, Préat V, Roberfroid MB. Phenobarbital as a promoter in the initiation/selection process of experimental rat hepatocarcinogenesis. Carcinogenesis 1983;4:141–144.
62. Bishayee A, Bhatia D, Thoppil RJ, Darvesh AS, Nevo E, Lansky EP. Pomegranate-mediated chemoprevention of experimental hepatocarcinogenesis involves Nrf2-regulated antioxidant mechanisms. Carcinogenesis 2011; 32:888–896.
63. Luther DL, Ohanyan V, Shamhart PE, et al. Chemopreventive doses of resveratrol do not affect cardiac function in a rodent model of hepatocellular carcinoma. Invest New Drugs 2011;29:380–391.
64. Kim W, Oe Lim S, Kim JS, et al. Comparison of proteome between hepatitis B virus- and hepatitis C virus-associated hepatocellular carcinoma. Clin Cancer Res 2003;9: 5493–5500.
65. Lim SO, Park SJ, Kim W, et al. Proteome analysis of hepatocellular carcinoma. Biochem Biophys Res Commun 2002;291:1031–1037.
66. Smith WL, Garavito RM, DeWitt DL. Prostaglandin endoperoxide H synthases (cyclooxygenases)-1 and -2. J Biol Chem 1996;271:33157–33160.
67. Pikarsky E, Porat RM, Stein I, et al. NF-kappaB functions as a tumour promoter in inflammation-associated cancer. Nature 2004;431:461–466.
68. Shishodia S, Aggarwal BB. Nuclear factor-kappaB activation: A question of life or death. J Biochem Mol Biol 2002;35:28–40.
69. Ghosh S, Karin M. Missing pieces in the NF-kappaB puzzle. Cell 2002;109:81–96.
70. Balkwill F, Mantovani A. Inflammation and cancer: Back to Virchow? Lancet 2001;357:539–545.
71. Roder DM. The epidemiology of gastric cancer. Gastric Cancer 2002;5:5–11.

72. Ekbom A. Risk of cancer in ulcerative colitis. J Gastrointest Surg 1998;2:312–313.
73. Pitot HC, Sirica AE. The stages of initiation and promotion in hepatocarcinogenesis. Biochim Biophys Acta 1980;605:191–215.
74. Lindquist S. The heat-shock response. Annu Rev Biochem 1986;55:1151–1191.
75. Morimoto RI. Cells in stress: Transcriptional activation of heat shock genes. Science 1993;259:1409–1410.
76. Lindquist S, Craig EA. The heat-shock proteins. Annu Rev Genet 1988;22:631–677.
77. Craig EA, Weissman JS, Horwich AL. Heat shock proteins and molecular chaperones: Mediators of protein conformation and turnover in the cell. Cell 1994;78:365–372.
78. Morimoto RI, Tisseres A, Georgopoulos C. Heat shock proteins in biology and medicine. New York: Cold Spring Harbor Press; 1994.
79. Scharf KD, Hohfeld I, Nover L. Heat stress response and heat stress transcription factors. J Biosci 1998;23:313–329.
80. Jolly C, Morimoto RI. Role of the heat shock response and molecular chaperones in oncogenesis and cell death. J Natl Cancer Inst 2000;92:1564–1572.
81. Mosser DD, Morimoto RI. Molecular chaperones and the stress of oncogenesis. Oncogene 2004;23:2907–2918.
82. Pascale RM, Simile MM, Calvisi DF, et al. Role of HSP90, CDC37, and CRM1 as modulators of P16(INK4A) activity in rat liver carcinogenesis and human liver cancer. Hepatology 2005;42:1310–1319.
83. Kaposi-Novak P, Lee JS, Gomez-Quiroz L, Coulouarn C, Factor VM, Thorgeirsson SS. Met-regulated expression signature defines a subset of human hepatocellular carcinomas with poor prognosis and aggressive phenotype. J Clin Invest 2006;116:1582–1595.
84. Boyault S, Rickman DS, de Reynies A, et al. Transcriptome classification of HCC is related to gene alterations and to new therapeutic targets. Hepatology 2007;45:42–52.
85. Nussbaum T, Samarin J, Ehemann V, et al. Autocrine insulin-like growth factor-II stimulation of tumor cell migration is a progression step in human hepatocarcinogenesis. Hepatology 2008;48:146–156.
86. Breinig M, Caldas-Lopes E, Goeppert B, et al. Targeting heat shock protein 90 with non-quinone inhibitors: A novel chemotherapeutic approach in human hepatocellular carcinoma. Hepatology 2009;50:102–112.
87. Carr BI, Huang TH, Buzin CH, Itakura K. Induction of heat shock gene expression without heat shock by hepatocarcinogens and during hepatic regeneration in rat liver. Cancer Res 1986;46:5106–5111.
88. Tacchini L, Schiaffonati L, Rappocciolo E, Cairo G, Bernelli-Zazzera A. Expression pattern of the genes for different members of the heat-shock protein 70 family, ornithine decarboxylase, and c-Ha-ras during the early stages of hepatocarcinogenesis. Mol Carcinog 1989;2:233–236.
89. Shiota G, Okubo M, Noumi T, et al. Cyclooxygenase-2 expression in hepatocellular carcinoma. Hepatogastroenterology 1999;46:407–412.
90. Cervello M, Montalto G. Cyclooxygenases in hepatocellular carcinoma. World J Gastroenterol 2006;12:5113–5121.
91. Koga H. Hepatocellular carcinoma: Is there a potential for chemoprevention using cyclooxygenase-2 inhibitors? Cancer 2003;98:661–667.
92. Kern MA, Haugg AM, Koch AF, et al. Cyclooxygenase-2 inhibition induces apoptosis signaling via death receptors and mitochondria in hepatocellular carcinoma. Cancer Res 2006;66:7059–7066.
93. Fodera D, D'Alessandro N, Cusimano A, et al. Induction of apoptosis and inhibition of cell growth in human hepatocellular carcinoma cells by COX-2 inhibitors. Ann NY Acad Sci 2004;1028:440–449.
94. Li J, Chen X, Dong X, Xu Z, Jiang H, Sun X. Specific COX-2 inhibitor, meloxicam, suppresses proliferation and induces apoptosis in human HepG2 hepatocellular carcinoma cells. J Gastroenterol Hepatol 2006;21:1814–1820.
95. Rahman MA, Dhar DK, Yamaguchi E, et al. Coexpression of inducible nitric oxide synthase and COX-2 in hepatocellular carcinoma and surrounding liver: Possible involvement of COX-2 in the angiogenesis of hepatitis C virus-positive cases. Clin Cancer Res 2001;7:1325–1332.
96. Marquez-Rosado L, Trejo-Solis MC, Garcia-Cuellar CM, Villa-Trevino S. Celecoxib, a cyclooxygenase-2 inhibitor, prevents induction of liver preneoplastic lesions in rats. J Hepatol 2005;43:653–660.
97. Hu KQ. Rationale and feasibility of chemoprevention of hepatocellular carcinoma by cyclooxygenase-2 inhibitors. J Lab Clin Med 2002;139:234–243.
98. Nakamura Y, Matsumoto H, Todoki K. Endothelium-dependent vasorelaxation induced by black currant concentrate in rat thoracic aorta. Jpn J Pharmacol 2002;89:29–35.
99. Iwasaki-Kurashige K, Loyage-Rendon RY, Matsumoto H, Tokunaga T, Azuma H. Possible mediators involved in decreasing peripheral vascular resistance with blackcurrant concentrate (BC) in hind-limb perfusion model of the rat. Vasc Pharm 2006;44:215–233.
100. Rosenblat M, Volkova N, Attias J, Mahamid R, Aviram M. Consumption of polyphenolic-rich beverages (mostly pomegranate and black currant juices) by healthy subjects for a short term increased serum antioxidant status, and the serum's ability to attenuate macrophage cholesterol accumulation. Food Funct 2010;1:99–109.
101. Courtois G, Gilmore TD. Mutations in the NF-kappaB signaling pathway: Implications for human disease. Oncogene 2006;25:6831–6843.
102. Hoffmann A, Baltimore D. Circuitry of nuclear factor kappaB signaling. Immunol Rev 2006;210:171–186.
103. Tazawa R, Xu XM, Wu KK, Wang LH. Characterization of the genomic structure, chromosomal location and promoter of human prostaglandin H synthase-2 gene. Biochem Biophys Res Commun 1994;203:190–199.
104. Rahman MA, Dhar DK, Masunaga R, Yamanoi A, Kohno H, Nagasue N. Sulindac and exisulind exhibit a significant antiproliferative effect and induce apoptosis in human hepatocellular carcinoma cell lines. Cancer Res 2006;60:2085–2089.
105. Calvisi DF, Pinna F, Ladu S, et al. Aberrant iNOS signaling is under genetic control in rodent liver cancer and potentially prognostic for the human disease. Carcinogenesis 2008;29:1639–1647.
106. Ueno S, Aoki D, Kubo F, et al. Roxithromycin inhibits constitutive activation of nuclear factor kappaB by diminishing oxidative stress in a rat model of hepatocellular carcinoma. Clin Cancer Res 2005;11:5645–5650.
107. Wu X, Beecher GR, Holden JM, Haytowitz DB, Gebhardt SE, Prior RL. Concentrations of anthocyanins in common foods in the United States and estimation of normal consumption. J Agric Food Chem 2006;54:4069–4075.
108. Bartoszek A. Genotoxic food components. In: Baer-Dubowska W, Brtoszek A, Malejka-Giganti D, editors. Carcinogenic and anticarcinogenic food components. Boca Raton: CRC Press; 2006. pp. 69–96.